221B Lecture Notes
Scattering Theory III

1 Partial Wave Analysis

1.1 Partial Wave Expansion

The scattering amplitude can be calculated in Born approximation for many interesting cases, but as we saw in a few examples already, we need to work out the scattering amplitudes more exactly in certain cases. The useful method is the partial wave analysis. When the potential is central, *i.e.*, spherically symmetric $V(\vec{r}) = V(r)$, angular momentum is conserved due to Noether's theorem. Therefore, we can expand the wave function in the eigenstates of the angular momentum. Obtained waves with definite angular momenta are called partial waves. We can solve the scattering problem for each partial wave separately, and then in the end put them together to obtain the full scattering amplitude.

The starting point is the asymptotic behavior of the wave function

$$\psi(\vec{x}) \sim e^{ikz} + f(\theta)\frac{e^{ikr}}{r}. \tag{1}$$

We use the formula shown in "Notes on Spherical Bessel Functions"

$$e^{ikz} = \sum_{l=0}^{\infty}(2l+1)i^l j_l(kr)P_l(\cos\theta). \tag{2}$$

The plane wave contains all values of l. This can be understood intuitively as follows. The plane wave is infinitely extended in all space. Therefore, in classical terms, it contains all values of the impact parameter b. For a fixed value of the momentum $p = \hbar k$, the angular momentum is $L = bp$ and hence it contains all values of the angular momentum $L = \hbar l$ with $l = bk$. It is useful later to write down the asymptotic behavior at large r using $j_l(kr) \sim \sin(kr - l\pi/2)/kr$,

$$e^{ikz} = \frac{1}{2ikr}\sum_{l=0}^{\infty}(2l+1)(e^{ikr} - (-1)^l e^{-ikr})P_l(\cos\theta). \tag{3}$$

It contains both the wave converging to the origin and the wave emerging from the origin, as intuition suggests.

Similarly, the 2nd term should be expanded in terms of the partial waves.

$$f(\theta) = \sum_{l=0}^{\infty}(2l+1)f_l P_l(\cos\theta). \tag{4}$$

All information on physics is contained in the complex numbers f_l. The factor $2l+1$ is for mere convenience.

1.2 Optical Theorem Constraint

The optical theorem places important constraints on f_l. Recall the optical theorem

$$\sigma = \int d\Omega |f|^2 = \frac{4\pi}{k}\Im f(0). \tag{5}$$

The l.h.s. is

$$
\begin{aligned}
\sigma &= \int d\Omega |f|^2 \\
&= 2\pi \int d\cos\theta \sum_{l,l'}(2l+1)(2l'+1)f_l f_{l'}^* P_l(\cos\theta)P_{l'}(\cos\theta) \\
&= 4\pi \sum_l (2l+1)|f_l|^2.
\end{aligned}
\tag{6}
$$

Here, normalization and orthogonality of the Legendre polynomials

$$\int_{-1}^{1} P_l(t)P_{l'}(t)dt = \frac{2}{2l+1}\delta_{l,l'} \tag{7}$$

was used. The r.h.s. of Eq. (5) is, on the other hand,

$$\frac{4\pi}{k}\Im f(0) = \frac{4\pi}{k}\sum_l(2l+1)(\Im f). \tag{8}$$

Here, I used the fact $P_l(\cos\theta) = 1$ for $\cos\theta = 1$. Comparing Eqs. (6) and (8), we find

$$|f_l|^2 = \frac{1}{k}\Im f_l \tag{9}$$

This is an important result. This constraint can be rewritten as

$$|1 + 2ikf_l|^2 = 1. \tag{10}$$

2

In other words, the combination $1 + 2ikf_l$ is just a phase

$$e^{2i\delta_l} = 1 + 2ikf_l \tag{11}$$

or equivalently,

$$f_l = \frac{e^{2i\delta_l} - 1}{2ik} = \frac{1}{k} e^{i\delta_l} \sin \delta_l. \tag{12}$$

The meaning of this phase δ_l becomes clearer shortly.

1.3 Phase Shifts

We write the asymptotic form Eq. (1) in terms of partial waves. It is

$$\psi(\vec{x}) \sim \sum_{l=0}^{\infty} (2l+1) i^l j_l(kr) P_l(\cos\theta) + \frac{e^{ikr}}{r} \sum_{l=0}^{\infty} (2l+1) f_l P_l(\cos\theta). \tag{13}$$

Using the asymptotic behavior $j_l(kr) \sim \sin(kr - l\pi/2)/kr$ and $f_l = e^{i\delta_l} \sin \delta_l/k$,

$$\psi(\vec{x}) \sim \frac{1}{kr} \sum_{l=0}^{\infty} (2l+1) P_l(\cos\theta) \left[i^l \sin\left(kr - l\frac{\pi}{2} \right) + e^{ikr} e^{i\delta_l} \sin \delta_l \right]. \tag{14}$$

The terms in the square bracket can be combined as

$$\psi(\vec{x}) \sim \frac{1}{2ikr} \sum_{l=0}^{\infty} (2l+1) P_l(\cos\theta) \left[e^{2i\delta_l} e^{ikr} - (-1)^l e^{-ikr} \right]. \tag{15}$$

Or in other words, the radial wave function behaves as

$$R_l(r) \sim \frac{1}{2ikr} \frac{1}{\sqrt{4\pi(2l+1)}} \left[e^{2i\delta_l} e^{ikr} - (-1)^l e^{-ikr} \right]. \tag{16}$$

(Here I used the normalization factor $Y_l^0(\theta, \phi) = \sqrt{(2l+1)/4\pi} P_l(\cos\theta)$, but the rest of the discussions does not depend on this factor.) This is an interesting equation. Compare it to the case of the plane wave without scattering Eq. (3). What this equation says is that the wave converging on the scatterer e^{-ikr} has the well-defined phase factor $-(-1)^l$, the same as in the case without scattering. This is because it comes from the expansion of the plane wave part only. On the other hand, the wave that emerges from the scatterer has an additional phase factor $e^{2i\delta_l}$. All what scattering did is to shift the

3

phase of the emerging wave by $2\delta_l$. The reason why this is merely a phase factor is the conservation of probability. What converged to the origin must come out with the same strength. But this shift in the phase causes the interference among all partial waves differ from the case without the phase shifts, and the result is not a plane wave but contains the scattered wave.

The phase factor is the so-called S-matrix element

$$S_l = e^{2i\delta_l}, \tag{17}$$

This is related to the T-matrix discussed earlier by

$$S = 1 + iT, \tag{18}$$

and hence

$$T_l = 2e^{i\delta_l}\sin\delta_l = 2kf_l. \tag{19}$$

The S-matrix includes the transmitted wave, while T-matrix removes it and keeps only the scattered wave. This notation of S- and T-matrix is used extensively in the time-dependent formulation of the scattering problem.

In terms of the phase shifts, the cross section is given by

$$\sigma = \frac{4\pi}{k^2}\sum_l (2l+1)\sin^2\delta_l. \tag{20}$$

Actual calculation of phase shifts is basically to solve the Schrödinger equation for each partial waves,

$$\left[-\frac{1}{r}\frac{d^2}{dr^2}r + \frac{l(l+1)}{r^2} + \frac{2m}{\hbar^2}V(r)\right]R_l(r) = k^2 R_l(r). \tag{21}$$

After solving the equation, we take the asymptotic limit $r \to \infty$, and write $R_l(r)$ as a linear combination of $j_l(kr)$ and $n_l(kr)$. The relative coefficients of j_l and n_l determines the phase shift δ_l, and hence the cross section.

1.4 Unitarity Limit

It is interesting that there is a maximum possible value for the cross section for each partial wave. From Eq. (20), the cross section for a given partial wave l is

$$\sigma_l = \frac{4\pi}{k^2}(2l+1)\sin^2\delta_l \leq \frac{4\pi}{k^2}(2l+1). \tag{22}$$

The maximum is obtained for the phase shift $\delta_l = \pm\pi/2$. This is called unitarity limit, as it is a consequence of the unitarity of the S-matrix.

This limit can be qualitatively understood in the following semi-classical argument. If you inject a particle with momentum p at the impact parameter b, it has angular momentum $L = pb$. On the other hand, the angular momentum is quantized in quantum mechanics, $L = \hbar l$. Let us say that the quantized angular momentum l corresponds roughly to the impact parameter $b = L/p$ for $\hbar l < L < \hbar(l+1)$, *i.e.*,

$$\frac{l}{k} \le b \le \frac{l+1}{k}. \tag{23}$$

Assuming that the particle gets scattered with 100% probability when entering this ring, the classical cross section would be

$$\pi \left(\frac{l+1}{k}\right)^2 - \pi \left(\frac{l}{k}\right)^2 = \pi \frac{2l+1}{k^2}. \tag{24}$$

The unitarity limit is roughly the same as this semi-classical argument except for a factor of four.

2   Hard Sphere Scattering

As an example of partial wave analysis, we first look at the hard sphere scattering, with the potential

$$V = \begin{cases} 0 & (r > a) \\ \infty & (r < a) \end{cases} \tag{25}$$

This potential represents an impenetrable ball, and mimics the classical image of scattering. Because of infinite potential within the radius a, Born approximation is clearly not appropriate. We resort to the partial wave analysis to work out cross sections. The infinite potential corresponds to the boundary condition

$$R_l(a) = 0 \tag{26}$$

for all l in solving the Schrödinger equation Eq. (21).

2.1 S-wave

At low momenta $k \ll 1/a$, the centrifugal barrier inhibits the particle from entering the region of the scatterer. Therefore the scattering occurs only for the $l = 0$ partial wave, or S-wave. We first analyze the S-wave only, which turns out to be particularly simple. The analysis below, however, applies also when k is large.

The Schrödinger equation Eq. (21) is simply that of a free particle in one dimension

$$\left[-\frac{d^2}{dr^2} + \frac{2m}{\hbar^2} V(r) \right] (rR_0(r)) = k^2(rR_0(r)), \tag{27}$$

with the boundary condition $rR_0 = 0$ at $r = a$. Therefore the solution is uniquely

$$rR(r) = c \sin(k(r - a)) = \frac{c}{2i} \left[e^{ikr-ika} - e^{-ikr+ika} \right], \tag{28}$$

where c is an overall normalization factor (in general complex).

To determine the phase shift, we compare this solution to the general expression Eq. (16)

$$R_0(r) \sim \frac{1}{2ikr} \frac{1}{\sqrt{4\pi}} \left[e^{2i\delta_0} e^{ikr} - e^{-ikr} \right], \tag{29}$$

and we find

$$\delta_0 = -ka. \tag{30}$$

The reason behind the phase shift is obvious. Because the wave cannot penetrate into $r < a$, the wave is shifted *outwards*, which is the shift in the phase $-ka$.

The cross section from the S-wave scattering is obtained from Eq. (20),

$$\sigma_0 = \frac{4\pi}{k^2} \sin^2 \delta_0 = \frac{4\pi}{k^2} \sin^2 ka. \tag{31}$$

The maximum cross section occurs at $k = 0$, where $\sigma_0 = 4\pi a^2$. This is four times larger than the classical geometric cross section πa^2, but at least of the same order of magnitude. The partial wave cross section saturates the unitarity limit where $ka = n\pi$, and keeps oscillating to higher momenta. The oscillating behavior merely signals the finite size of the target. However, the persistent oscillation up to infinite momentum is because of the oversimplification of impenetrable sphere with a rigid surface.

Because this analysis is so simple, let us generalize the discussion to the case of a little bit penetrable potential

$$V = \begin{cases} 0 & (r > a) \\ V_0 & (r < a) \end{cases} \tag{32}$$

We use the notation $K^2 = 2mV_0/\hbar^2$. First consider the situation $k > K$. We then find

$$rR = \begin{cases} \sin(\sqrt{k^2 - K^2}\, r) & r < a \\ \sin(ka + \delta_0) & r > a \end{cases}. \tag{33}$$

By matching the logarithmic derivatives of the wave function at $r = a$, we find

$$\frac{(rR)'}{rR} = \sqrt{k^2 - K^2} \cot(\sqrt{k^2 - K^2}\, a) = k \cot(ka + \delta_0), \tag{34}$$

or

$$\delta_0 = \tan^{-1}\left[\frac{k}{\sqrt{k^2 - K^2}} \tan(\sqrt{k^2 - K^2}\, a)\right] - ka. \tag{35}$$

For $k \gg K$, one can neglect K and the phase shift vanishes. The energy is too large to care the slight potential and there is no scattering any more. Therefore the partial wave cross section does not saturate the unitarity limit at $k \gg K$ and asymptotes to zero.

On the other hand, for small $k < K$, the wave function is

$$rR = \begin{cases} \sinh(\sqrt{K^2 - k^2}\, r) & r < a \\ \sin(ka + \delta_0) & r > a \end{cases}. \tag{36}$$

The phase shift is obtained as

$$\delta_0 = \tan^{-1}\left[\frac{k}{\sqrt{K^2 - k^2}} \tanh(\sqrt{K^2 - k^2}\, a)\right] - ka. \tag{37}$$

At small $k \ll K$, it can further be expanded as

$$\delta_0 \sim ka\left[\frac{1}{Ka} \tanh Ka - 1\right]. \tag{38}$$

The quantity in the square bracket is always between 0 and -1, and hence the cross section is at most that of the hard sphere. This makes sense intuitively. Another interesting point is that the phase shift δ_0 always starts linearly with

7

k at small momentum, and the slope is *negative*. This is a completely general result for a repulsive potential, and a convenient quantity

$$a_0 = -\lim_{k \to 0} \frac{d\delta_0}{dk} \tag{39}$$

is called the *scattering length*, as it has the dimension of the length. This quantity basically measures how big the scatterer is. The cross section at $k \to 0$ limit is then given by $4\pi a_0^2$. For the hard sphere potential, the scattering length is indeed the size of the sphere.

This example basically demonstrates that the cross section of α particle off an atom, which we discussed within Born approximation before, cannot be much larger than the geometric cross section given by the size of the atom despite what Born approximation suggested for $k \ll a^{-1}$.

2.2 Higher Partial Waves

For the hard sphere problem, the phase shifts for higher partial waves can be worked out also easily. For $r > a$, the Schrödinger equation is again that of the free one, and hence the solution is a linear combination of j_l and n_l,

$$
\begin{aligned}
R_l &\propto j_l(kr)\cos\theta + n_l(kr)\sin\theta \\
&\sim \sin\left(kr - \frac{\pi}{2}l\right)\cos\theta + \cos\left(kr - \frac{\pi}{2}l\right)\sin\theta = \sin\left(kr - \frac{\pi}{2}l + \theta\right)
\end{aligned} \tag{40}
$$

Comparing this asymptotic form at $r \gg a$ to the definition of the phase shift

$$R_l \propto e^{2i\delta_l}e^{ikr} - (-1)^l e^{-ikr} = e^{i\delta_l}i^l 2i\sin\left(kr - \frac{\pi}{2}l + \delta_l\right), \tag{41}$$

θ above is nothing but the phase shift δ_l.[1] Then we require that the wave function vanishes at $r = a$:

$$R_l(a) \propto j_l(ka)\cos\delta_l + n_l(ka)\sin\delta_l = 0. \tag{42}$$

Therefore we find

$$\tan\delta_l = -\frac{j_l(ka)}{n_l(ka)}, \tag{43}$$

---

[1] I've just noticed that my notation for n_l differs from Sakurai's by a sign as seen in Eq. (7.6.52) on page 409. I'm sorry for that, but to keep consistency with my notes on spherical bessel functions, I stick with my convention, which was taken from Messiah.

or

$$e^{2i\delta_l} = \frac{h_l^{(-)}(ka)}{h_l^{(+)}(ka)}. \tag{44}$$

For small momenta $k \ll a^{-1}$, it is straightforward to show that $\delta_l \propto k^{2l+1}$, and hence is smaller for higher partial waves. This is easy to understand. When k is small, the centrifugal barrier $-\hbar^2 l(l+1)/r^2$ does not allow particle to reach $r = a$ classically, and only the exponential tail of the wave function reaches $r = a$. Therefore the effect of the potential is extremely suppressed.

On the other hand at high monenta, $\sin^2 \delta_l$ oscillates between 0 and 1 as a function or l up to $l \simeq ka$. Above this value, the phase shift drops rapidly to zero. This makes sense from the classical physics intuition. When $l \geq ka$, the impact parameter is larger than the size of the target $b \geq a$ and there shouldn't be any scattering. This behavior of the phase shift leads to the total cross section or $2\pi a^2$ at high momenta.

3 Attractive Potential

The potential Eq. (32) can also be an attractive potential if $V_0 < 0$. The phase shift for this case can be easily obtained from Eq. (35) by changing the sign of $K^2 = -2mV_0/\hbar^2$,

$$\delta_0 = \tan^{-1} \left[\frac{k}{\sqrt{k^2 + K^2}} \tan(\sqrt{k^2 + K^2}\, a) \right] - ka. \tag{45}$$

The first interesting feature of this phase shift is that it can start with a *positive* slope unlike the repulsive case. The scattering length is

$$a_0 = -\left. \frac{d\delta_0}{dk} \right|_{k=0} = a \left[1 - \frac{\tan Ka}{Ka} \right]. \tag{46}$$

For small K, the scattering length is negative, *i.e.*, the opposite sign of the repulsive case. This is easy to understand because the wave is pulled into the potential rather pushed out unlike the repulsive case. However, once we make the potential more attractive (larger K), the scattering length grows and becomes even infinite at $K = \pi/2$! What is going on?

To answer this question, let us study the analytic structure of the scattering amplitude more carefully. From Eq. (45), we can write

$$e^{2i\delta_0} = e^{-2ika} \frac{1 + i\frac{k}{\sqrt{k^2+K^2}} \tan(\sqrt{k^2 + K^2}\, a)}{1 - i\frac{k}{\sqrt{k^2+K^2}} \tan(\sqrt{k^2 + K^2}\, a)} \tag{47}$$

9

This S-matrix element can have a pole if

$$1 - i\frac{k}{\sqrt{k^2 + K^2}}\tan(\sqrt{k^2 + K^2}\,a) = 0. \tag{48}$$

This equation appears impossible to satisfy, but it can be on the complex plane of k. For a pure imaginary $k = i\kappa$, the equation becomes

$$\kappa = -\frac{\sqrt{K^2 - \kappa^2}}{\tan(\sqrt{K^2 - \kappa^2}\,a)}. \tag{49}$$

This is nothing but the condition for bound states. By decreasing K from a sufficiently large value with bound state(s), the bound state energies $E = -\hbar^2\kappa^2/2m$ move up. When $Ka = (n + \frac{1}{2})\pi$, $\tan Ka = \infty$, and we find a bound state approaching $\kappa = k = 0$. This is when the scattering length diverges in Eq. (46). In other words, the infinite scattering cross section at $k = 0$ happens because there is a bound state exactly at $k = 0$. If you further decrease K, the bound state completely disappears. However the cross section for small k remains very large, not quite $4\pi^2/k^2$ as allowed by unitarity, but much bigger than $4\pi^2 a^2$.

This can also be seen on the complex k plane in the following manner. The lower half plane is unphysical as it corresponds to an exponentially growing wave function at the infinity for the scattered wave e^{ikr}. When there are bound states, you see poles along the positive imaginary axis. By decreasing K, the poles along the positive imaginary axis go down, and a pole reaches the origin. By further decreasing K, the pole goes below the origin into the unphysical region. However, the existence of a pole just below the origin makes the scattering amplitude at $k \sim 0$ large and results in an anomalously large cross section.

On the other hand, the phase shift Eq. (45) can be multiples of $n\pi$ for special values of k. Even though the particle passes through a potential, the wave oscillates precisely integer of half-integer times in the potential in addition to the free particle phase and there is no cross section. This phenomenon is called Ramsauer–Townsend effect, which had been observed in the scattering of electrons by rare gas atoms and was a great mystery before Bohr proposed the wave description.

A good example of large cross sections close to the threshold is the neutron scattering cross section off large nuclei. The cross section can be many orders of magnitude larger than the geometric size of nuclei. This is why slow
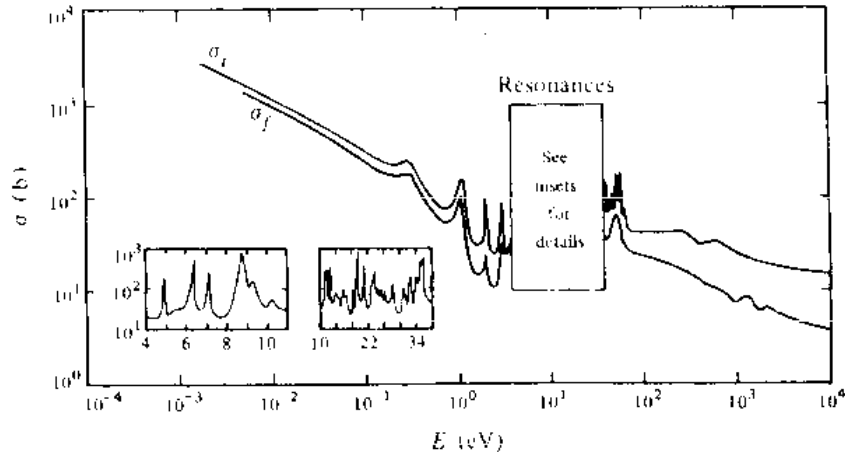
Fig. 17.5. Total (σ_t) and fission (σ_f) cross sections of ^{235}U. (1 b = 10^{-24} cm^2.)

Figure 1: Neutron cross section that shows a large enhancement close to the threshold and many resonances above the treshold. Taken from *Subatomic Physics*, Hans Frauenfelder and Ernest M. Henley, Prentice-Hall, Inc., 1974.

neutrons can be effectively absorbed by Uranimum in nuclear power plants to cause further fission processes in a chain reaction, and similarly in atomic bombs.

4   Resonances

The attractive spherical well potential discussed in the previous section led to possible large cross sections close to the threshold $k \sim 0$. Can one obtain large cross sections away from the threshold? One can, if there are "resonances."

Recall that the poles in the unphysical lower half plane in k were responsible for large cross section near the threshold. This pole corresponds to a would-be bound state. Similarly a pole just below the real axis would lead to a large cross section. They must also correspond to some sort of "bound states." What are they?

There are few examples of potential that can be worked out simply and exhibit resonances. Here we discuss an idealized potential called "delta-shell"

11

potential,

$$V(r) = \gamma\delta(r - a). \tag{50}$$

This potential leads to a true bound state if γ is sufficiently negative. On the other hand, for $\gamma \to \infty$, the regions inside $r < a$ and outside $r > a$ the potential are decoupled and one finds a tower of states confined inside the shell. The fate of these states for finite γ is very interesting.

The phase shift for the S-wave can be worked out analytically,

$$e^{2i\delta_0} = \frac{1 + \frac{2m\gamma}{\hbar^2 k}e^{-ika}\sin ka}{1 + \frac{2m\gamma}{\hbar^2 k}e^{ika}\sin ka} = e^{-2ika}\frac{\sin ka + \frac{\hbar^2 k}{2m\gamma}e^{ika}}{\sin ka + \frac{\hbar^2 k}{2m\gamma}e^{-ika}}. \tag{51}$$

We now look for poles of the denominator, which can be rewritten as

$$e^{2ika} = 1 - 2i\frac{\hbar^2 k}{2m\gamma}. \tag{52}$$

When γ is large, the second term is small, and we find $2ika = 2\pi in$, or $ka = n\pi$. Given the correction, we want to solve

$$2ika = \log\left(1 - 2i\frac{\hbar^2 k}{2m\gamma}\right) + 2in\pi. \tag{53}$$

Expanding the logarithm up to $O(k^2)$ and solving the quadratic equation, we obtain

$$k \simeq \frac{n\pi}{a + \frac{\hbar^2}{2m\gamma}} - i\left(\frac{\hbar^2}{2m\gamma}\right)^2\frac{(n\pi)^2}{a^3} + O(\gamma)^{-2} \tag{54}$$

The poles are in the unphysical lower half plane. But when γ is large, the poles are very close to the real axis, and the scattering amplitude receives a large enhancement due to these poles.

What are these poles? Unlike the poles along the positive imaginary axis, which represent real bound states, these poles are unphysical. However in the limit of $\gamma \to 0$, or in other words in the limit of small coupling between the regions inside and outside the shell, they become poles along the real axis. They are the discrete states inside the shell in this limit. By making γ finite, you introduce coupling between the discrete states inside the shell to the continuum states outside the shell. Therefore it is still useful to find "physical" interpretations of the unphysical poles.

For this purpose, it is instructive to solve Schrödinger equation for the values of k which correspond to the location of poles satisfying Eq. (52). The solutions can be found in a straight-forward way

$$rR_0(r) = \begin{cases} \sin kr & (r < a) \\ \sin ka \, e^{ik(r-a)} & (r > a) \end{cases} \tag{55}$$

Because the factor $e^{ik(r-a)}$ grows expontentially at large r due to the negative imaginary part in k, the solution is not a regular normalizable solution. But nonetheless let us proceed. In the large γ limit, polease are given in Eq. (54) and $\sin ka \sim O(\gamma)^{-1}$ is small. Therefore the wave function almost vanishes at the shell. Out side the shell, the wave function oscillates at the small amplitude $\sin ka$, which however starts growing again due to the $e^{ik(r-a)}$ factor exponentially. We now put the time dependence in. The energy eigenvalue is nothing but $E = \hbar^2 k^2/2m$, where k is at the pole. If the pole is at

$$k = k_0 - i\kappa \tag{56}$$

the energy eigenvalue is at

$$E = E_0 - i\frac{\Gamma}{2} = \frac{\hbar^2 k_0^2}{2m} - i\frac{\hbar^2 k_0 \kappa}{m} + O(\kappa^2). \tag{57}$$

For instance in the large γ limit, the poles given in Eq. (54) give

$$E = E_0 - i\frac{\Gamma}{2} \sim \frac{\hbar^2}{2m}\left(\frac{n\pi}{a + \frac{\hbar^2}{2m\gamma}}\right)^2 - i\left(\frac{\hbar^2 n\pi}{2ma}\right)^3 \frac{2}{\gamma^2 a} + O(\gamma)^{-3}. \tag{58}$$

The time dependence of the wave function is simply

$$rR_0(r,t) = rR_0(r)e^{-iEt/\hbar} = rR_0(r)e^{-iE_0t/\hbar}e^{-\Gamma t/2\hbar}. \tag{59}$$

Overall, the wave function is then

$$rR_0(r,t) = \begin{cases} \sin kr \, e^{-iE_0t/\hbar}e^{-\Gamma t/2\hbar} & (r < a) \\ \sin ka \, e^{ik(r-a)}e^{-iE_0t/\hbar}e^{-\Gamma t/2\hbar} & (r > a) \end{cases} \tag{60}$$

This is a very interesting result. Inside the shell, it shows an exponentially decaying probability density $|rR_0(r,t)|^2 \propto e^{-\Gamma t/\hbar}$ uniformly over space. Outside the shell, the probability density is $|rR_0(r,t)|^2 \propto e^{2\kappa r}e^{-\Gamma t/\hbar}$, which

13

shows the probability flowing out to inifinity with speed $\Gamma/2\hbar\kappa = \hbar k_0/m$, nothing but the velocity of the particle itself. In other words, the wave function describes a "bound state" inside shell decaying into a continuum state outside the shell moving away at the expected velocity (a "run-away" wave). Even though the pole is certainly in the "unphysical" region, this interpretation makes it quite physical at least in the limit of large γ or small coupling between the discrete and continuum states. The resonances can be viewed as quasi-bound states which decay into continuum states. The lifetime of the quasi-bound states is $\tau = \hbar/\Gamma$.

Is the complex energy eigenvalue allowed? You have been repeatedly told that a Hermitean operator, such as Hamiltonian, has only real eigenvalues. However, this statement is true for normalizable wave functions, because the proof crucial depends on the integration by parts and for unnormalizable wave functions integral themselves are ill-defined. Once one allows an exponentially growing wave function, the ordinary proof of real eigenvalues breakd down, and one can find complex eigenvalues.

In fact, all excited states of an atom appear as resonances in the photon-atom scattering. In the limit of turning off the coupling of photons to the electron, the excited states are all stable bound states. But the coupling (albeit small thanks to $\alpha = 1/137 \ll 1$) lets the excited state decay into the continuum states of photons.

In general, once we know that there is a pole just below the real axis, we can approximate the S-matrix by the contribution from the pole only, ignoring a continuum. Note that this approximation is good only if the pole is close to the real axis. Then as a function of the energy, S-matrix element is approximated as

$$S_l = e^{2i\delta_l} \simeq \frac{g(E)}{E - E_0 + i\Gamma/2}. \tag{61}$$

Because of the unitarity $|S|^2 = 1$, we immediately conclude

$$S_l = e^{2i\delta_l} \simeq \frac{E - E_0 - i\Gamma/2}{E - E_0 + i\Gamma/2}. \tag{62}$$

Then

$$\sin^2 \delta_l = \frac{\Gamma^2}{(E - E_0)^2 + \Gamma^2/4}. \tag{63}$$

At $E = E_0$, it saturates the unitarity limit $\sin^2 \delta_l = 1$, and it has a Lorenzian shape in terms of the energy. Γ is nothing but the FWHM (Full-Width-Half-Maximum) of the Lorentzian peak in $\sin^2 \delta_l$. Cross section is $\sigma = (4\pi/k^2)(2l+$

1) $\sin^2 \delta_l$ as usual. Comparing the discussion of the decaying probability density with a run-away wave and the dependence of the cross section on the energy, we established the relationship between the life time of the quasi-bound state τ and the FWHM of the resonance Γ as $\tau = \hbar/\Gamma$. This is an explicit manifestation of the energy-time uncertainty relation $\Delta E \Delta t \gtrsim \hbar$.

Another interesting point is that the real part of the energy eigenvalue for the resonances is shifted from the limit $\gamma \to 0$. In other words, the fact that the quasi-bound state can decay into continuum changes the energy of the quasi-bound state due to the coupling to the continuum. In fact, the energies of the excited states of an atom are different from the energies calculated without considering the decay and the difference has to be included given the high accuracy of atomic physics experiments.

Coming back to the real energy eigenvalue and the delta-shell potential, the wave function is given by

$$rR_0(r) = \begin{cases} \frac{\sin(ka+\delta_0)}{\sin(ka)} \sin(kr) & r < a \\ \sin(kr + \delta_0) & r > a \end{cases}. \tag{64}$$

From Eq. (51), we find

$$\delta_0 = -ka + \arg\left[\sin ka + \frac{\hbar^2 k}{2m\gamma} e^{ika}\right]. \tag{65}$$

For most values of ka, the second term in the square bracket is negligible and the second term vanishes. Therefore the result is approximately the same as the hard sphere. Inside the shell, the prefactor $\sin(ka + \delta_0)$ is basically zero. In other words, the wave does not enter the shell. On the other hand, for special values $ka = 2n\pi$, the second term in the square bracket quickly moves from 0 to π (and π to 2π for $ka = (2n-1)\pi$). Only for these values of k, the prefactor $\sin(ka + \delta_0)/\sin(ka)$ can be sizable, but at most unity. The wave, therefore, *enters* the shell only for the "resonant" values of k.

5   Wave Packet with a Resonance

5.1   Separation of the Phase Shift

The main point of the analysis is that the S-matrix can be decomposed to two pieces

$$
\begin{aligned}
e^{2i\delta_0} &= e^{-2ika}\frac{\sin ka + \frac{\hbar^2 k}{2m\gamma}e^{ika}}{\sin ka + \frac{\hbar^2 k}{2m\gamma}e^{-ika}} \\
&= e^{-2ika} + e^{-2ika}\frac{\hbar^2 k}{2m\gamma}\frac{2i\sin ka}{\sin ka + \frac{\hbar^2 k}{2m\gamma}e^{-ika}}.
\end{aligned}
\tag{66}
$$

The first term is that of the hard sphere scattering, and its behavior can be analyzed very easily. The second term is dominated by the pole, which we can extract.

The wave function we obtained earlier in the lecture note is

$$
\psi(r) \equiv rR_0(r) = \begin{cases} \frac{\sin(ka+\delta_0)}{\sin(ka)}\sin(kr) & r < a \\ \sin(kr + \delta_0) & r > a \end{cases}.
\tag{67}
$$

To match with the general asymptotic form for the scattered wave $e^{ikr}e^{2i\delta_0} - e^{-ikr}$, we multiply the wave function, both inside and outside the shell, by $2ie^{i\delta_0}$ to find

$$
\psi(r) = \begin{cases} \frac{e^{ika}e^{2i\delta_0}-e^{-ika}}{\sin(ka)}\sin(kr) & r < a \\ e^{ikr}e^{2i\delta_0} - e^{-ikr} & r > a \end{cases}.
\tag{68}
$$

The wave packet is

$$
\psi = \int dq\, e^{-(q-k)^2 d^2}\left[e^{iqr}e^{2i\delta_0} - e^{-iqr}\right]e^{-i(\hbar q^2/2m)t}.
\tag{69}
$$

5.2   Hard Sphere Piece

Using the first term in Eq. (66), it is

$$
\psi = \int dq\, e^{-(q-k)^2 d^2}\left[e^{iqr}e^{-2iqa} - e^{-iqr}\right]e^{-i(\hbar q^2/2m)t}.
\tag{70}
$$

The stationary phase approximation is valid when t is moderately large (*i.e.*, large enough that $e^{-i(\hbar q^2/2m)t}$ factor oscillates rapidly while not too large for

the wave packet to start spreading). The stationary phase condition is

$$\frac{\partial}{\partial q}\left(-qr - \frac{\hbar q^2}{2m}t\right) = -r - \frac{\hbar q}{m}t = 0, \tag{71}$$

for the first term in the square bracket. This is nothing but the incoming wave packet located at $r = -(\hbar q/m)t$. Similarly the stationary phase condition for the second term in the square bracket is

$$\frac{\partial}{\partial q}\left(qr - 2qa - \frac{\hbar q^2}{2m}t\right) = r - 2a - \frac{\hbar q}{m}t = 0, \tag{72}$$

which is nothing but the scattered wave packet located at $r = (\hbar q/m)t + 2a$. Note that the term $2a$ tells us that the wave packet had not entered the shell but was bounced right by the shell.

The rest of the analysis is the same as before. We expand q around k as

$$qr - 2qa - \frac{\hbar q^2}{2m}t = kr - 2ka - \frac{\hbar k^2}{2m}t + (r - 2a - vt)(q - k) + O(q - k)^2, \tag{73}$$

ignore the second order correction, and integrate. We defined $v = \hbar k/m$ which is the velocity of the wave packet. Let us work out the behavior at large $t > 0$ for later use. Then only the first term in the square bracket in Eq. (69) contributes, and we find

$$\begin{aligned}
\psi &\simeq e^{ikr}e^{-2ika}e^{-i(\hbar k^2/2m)t}\int dq e^{-(q-k)^2 d^2}e^{i(r-2a-vt)(q-k)}\\
&= e^{ikr}e^{-2ika}e^{-i(\hbar k^2/2m)t}\frac{\sqrt{\pi}}{d}e^{-(r-2a-vt)^2/4d^2}.
\end{aligned} \tag{74}$$

5.3 Resonance Piece Outside the Shell

The interest is really in the second term in Eq. (66). Therefore the piece of our interest from Eq. (69) is

$$\psi = \int dq e^{-(q-k)^2 d^2}e^{iqr}e^{-2iqa}\frac{\hbar^2 q}{2m\gamma}\frac{2i\sin qa}{\sin qa + \frac{\hbar^2 q}{2m\gamma}e^{-iqa}}e^{-i(\hbar q^2/2m)t}. \tag{75}$$

First of all, it is small, suppressed by γ. Second, it has a pole. Assuming that the momentum range $q = k \pm d^{-1}$ contains only one of the resonances, but

17

d^{-1} much wider than the width of the resonance, we can study its behavior approximately as follows.

First of all, due to the pole at the resonance close to the real axis, the integral is dominated by the region around the pole. Let us call the location of the pole to be $k_0 - i\kappa$. Since the Gaussian factor is much wider than the resonance peak, we can approximate the Gaussian factor by a constant, namely $e^{-(k-k_0)^2 d^2}$. The phase factors can also be approximated at $q = k_0 + q'$ up to the linear order in q'. Then the integral is approximately

$$
\begin{aligned}
\psi &= e^{-(k-k_0)^2 d^2} e^{ik_0 r} e^{-2ik_0 a} e^{-i(\hbar k_0^2 / 2m)t} \\
&\int dq' \frac{\hbar^2 q}{2m\gamma} e^{iq'(r-2a-vt)} \frac{2i \sin qa}{\sin qa + \frac{\hbar^2 q}{2m\gamma} e^{-iqa}}.
\end{aligned}
\tag{76}
$$

Because the integrand is damped strongly as q' deviates from zero, we can pretend that the integration is from $-\infty$ to ∞. The point then is that one can extend the contour to go back at the infinity on the upper or lower half plane depending on the coefficient of iq' in the exponent is positive or negative, respectively. The contour in the upper half plane does not enclose any pole, and hence the integral vanishes. Therefore the integral is non-vanishing only if the coefficient of iq' in the exponent is negative, *i.e.*, for $t > (r - 2a)/v$. The contribution is there only *after* the scattering takes place, a resonable result. The important point is that the result of the integral would be just the substitution of $q' = -i\kappa$ or $q = k_0 - i\kappa$ in the integrand (except the denominator), which is basically

$$
e^{iqr} \sin qa e^{-i(\hbar q^2/2m)t}
\tag{77}
$$

evaluated at $q = k_0 - i\kappa$. This is precisely the form of the wave function we obtained for the complex momentum at the pole! In other words the large t behavior of the scattered wave is nothing but the "resonance wave function" for a complex energy eigenvalue. However, there is one notable difference. The contribution exists only for $(\hbar k_0/m)t > r - a$. The exponential rise of the resonance wave function e^{iqr} becomes appreciable only for $r > \kappa^{-1}$, which requires $t > \kappa^{-1}(m/\hbar k_0) = 2\hbar/\Gamma$. In other words, by the time exponential rise starts to show, the exponential decay $e^{-\Gamma t/2\hbar}$ sets in. The exponential therefore never becomes a true enhancement. The pathological non-renormalizability of the resonance wave function is hence a non-issue.

To work out more detailed form of the wave packet, let us perform the integration explicitly. Around the pole $q = k_0 - i\kappa$, we expand the denominator

as

$$\sin qa + \frac{\hbar^2 q}{2m\gamma} e^{-iqa} = 0 + \left(\cos qa + \frac{\hbar^2}{2m\gamma} e^{-iqa} - ia \frac{\hbar^2 q}{2m\gamma} e^{-iqa} \right) (q - k_0 + i\kappa)$$
$$+\text{higher order.} \tag{78}$$

Once we know how we pick the contribution of the pole, it is easier to go back to Eq. (75) to perform the integration. It gives

$$\psi = -2\pi i e^{-(q-k)^2 d^2} e^{iq(r-2a)} \frac{\hbar^2 q}{2m\gamma} \frac{2i\sin qa}{\cos qa + \frac{\hbar^2}{2m\gamma} e^{-iqa} - ia \frac{\hbar^2 q}{2m\gamma} e^{-iqa}} e^{-i(\hbar q^2/2m)t} \Bigg|_{q=k_0-i\kappa} . \tag{79}$$

By further using the condition for the pole, $\sin qa$ in the numerator can be rewritten as $-\frac{\hbar^2 q}{2m\gamma} e^{-iqa}$. Also, to a good approximation (large γ), $k_0 = n\pi/a + O(\gamma^{-1})$, $\kappa = O(\gamma^{-2})$ and hence $e^{-iqa} = \cos qa = (-1)^n + O(\gamma^{-1})$ and $\sin qa = O(\gamma^{-1})$. Putting them together, we find

$$\psi = -4\pi e^{-(q-k)^2 d^2} e^{iq(r-2a)} e^{-i(\hbar q^2/2m)t} \left(\frac{\hbar^2 q}{2m\gamma} \right)^2 \Bigg|_{q=k_0-i\kappa} \theta(vt - r - 2a). \tag{80}$$

We resurrected the condition $vt - r - 2a > 0$ for this contribution to exist.

5.4 Total Wave Packet Outside the Shell

The wave packet after the scattering is the sum of Eqs. (74) and (80) and we find

$$\psi \simeq \theta(vt - r - 2a) \left[e^{ik(r-2a)} e^{-i(\hbar k^2/2m)t} \frac{\sqrt{\pi}}{d} e^{-(r-2a-vt)^2/4d^2} \right.$$

$$\left. -4\pi e^{-(q-k)^2 d^2} e^{iq(r-2a)} e^{-i(\hbar q^2/2m)t} \left(\frac{\hbar^2 q}{2m\gamma} \right)^2 \Bigg|_{q=k_0-i\kappa} \right]. \tag{81}$$

The first term is peaked around $r = 2a + vt$ with a width of d and is the bounced back wave packet by the hard sphere. The second term is the "resonance wave function" starting at $r = 2a + vt$ with an exponential tail behind due to $e^{iqr} = e^{ik_0 r + \kappa r}$ factor. Therefore the total wave packet consists of a Gaussian peak followed by an exponential tail. Another way to look at it

19

is by placing a detector at a fixed r. Then at $t = (r+2a)/v$ you see the prompt peak followed by an exponential tail due to $|e^{-i(\hbar q^2/2m)t}|^2 = e^{-2(\hbar k_0 \kappa/m)t}$ factor. The physical interpretation of the exponential tail is precisely that of an exponentially decaying quasi-bound state. The relative phase between two terms is also important. Because we are interested in a wave packet whose momentum is peaked around the resonance $k = k_0$, the Gaussian factor $e^{-(q-k)^2 d^2}$ is basically unity, and all phase factors are the same between two terms. Therefore, there is a *destructive* interference. This is precisely what we need, because the exponential tail takes away some probability out of the bounced back wave packet, which requires the bounced back portion to be reduced to conserve probability.

5.5   Wave Packet Inside the Shell

The wavefunction inside the shell is

$$\psi = \int dq e^{-(q-k)^2 d^2} \frac{e^{iqa}e^{2i\delta_0} - e^{-iqa}}{\sin(qa)} \sin(qr)e^{-i(\hbar q^2/2m)t}. \tag{82}$$

Using the separation Eq. (66), the first term identically vanishes. Therefore it is only the second term we need to consider:

$$\psi = \int dq e^{-(q-k)^2 d^2} e^{-iqa} \frac{\hbar^2 q}{2m\gamma} \frac{2i}{\sin qa + \frac{\hbar^2 q}{2m\gamma}e^{-iqa}} \sin(qr)e^{-i(\hbar q^2/2m)t}. \tag{83}$$

Because the integrand is peaked highly around $q = k_0$, we can ignore the Gaussian factor as before.

The rest of the analysis is the same as the outside region. We approximate the phase factor with $q = k_0 + q'$ up to the linear order in q', and pretend that the integration is for the entire real axis. For a sufficiently large t, we can extend the contour to come back on the lower half plane, picking up the pole. Then the result is just the substitution of $q = k_0 - i\kappa$ in the integrand (except for the denominator), which is basically

$$\sin(qr)e^{-i(\hbar q^2/2m)t} \tag{84}$$

evaulated at the pole. Again, this is the "resonance wave function" we solved for a complex energy eigenvalue.

In sum, the wave packet behaves as follows. The wave packet has the velocity $v = \hbar k_0/m$. For $t < -a/v$, until the wave packet reaches the shell,

it consists of only one wave packet located at $r = -vt$. For large $t > -a/v$, the wave packet consists of three pieces. One of them is just the wave packet bounced back by the shell, moving along at $r = vt + 2a$. Two other pieces are coming from the resonance, inside and outside the shell. Both of them are well described by the "resonance wave function" obtained by solving the Schrödinger equation with a complex energy eingenvalue, damping exponentially as a function of time. In other words, after the main part of the wave packet is bounced back by the shell, a small portion remains, hangs around for a while, and starts decaying only over the time scale given by the lifetime of the quasi-bound state.

6   Examples

It is interesting to also consider the case where $\Delta q = d^{-1}$ is much smaller than the width of the resonance. In that case, the wave packet is so long that the "delayed" wave packet coming from the decay of the quasi-bound state overlaps with the bounced wave packet and we cannot separate them. Such an experiment will see the Breit–Wigner shape of the resonance as a function of the energy.

An example is the production of the Z^0 boson at LEP e^+e^- collider. The energy resolution of the beam is much smaller than the width of the Z^0 boson and hence it shows the Breit–Wigner shape of the resonance as a function of the center-of-mass energy. This experiment achieved an unprecedented accuracy in high-energy physics, resulting in the determination of the mass and the width of the Z^0 boson as

$$m_Z = 91.1875 \pm 0.0021 \text{GeV}, \tag{85}$$
$$\Gamma_Z = 2.4952 \pm 0.0023 \text{GeV}. \tag{86}$$

The data is shown in Fig. 2 from `http://arXiv.org/abs/hep-ex/0101027`.

In the same experiment, one can see the exponential decay law of particles produced from the Z^0 decay. Fig. 3 shows an example from `http://arXiv.org/abs/hep-ex/0011083`. Here, the Z^0 boson decays into a pair of bottom quarks, and they form bound states with another quark, such as u and d due to quark confinement into mesons B^0 and B^-. These mesons are very short-lived $\tau_{\bar{B}^0} = 1.518 \pm 0.053 \pm 0.034$ ps, $\tau_{B^-} = 1.648 \pm 0.049 \pm 0.035$ ps. However, in the decay of the Z^0 boson, they are boosted relativistically because the energy is $E_B = m_Z c^2 / 2 = 45.$ GeV while their masses are about
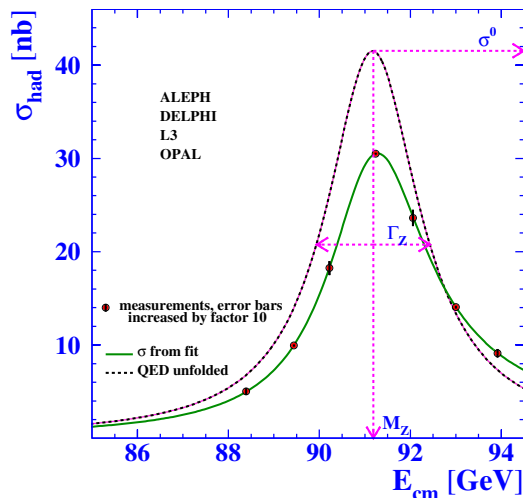
Figure 2: Average over measurements of the hadronic cross-sections by the four expeiments, as a function of centre-of-mass energy. The dashed curve shows the QED deconvoluted cross-section, which defines the Z parameters described in the paper.

5.279 GeV/c^2. The life time is hence prolonged by time dilation effect by $\gamma \sim 45.59/5.279 = 8.636$ (in practice this number is somewhat smaller because a b-quark jet produces other particles than the B-meson and they share energies). Furthermore, they run with a speed very close to the speed of light, and go for a distance of $l = c\tau\beta\gamma \simeq 0.415$ cm! This is a detectable distance using modern solid state detectors. The mesons decay into lighter mesons, in this case D-mesons. What you detect is further decay products of D-mesons. Extrapolating the tracks of the decay products back towards the e^+e^- annihilation point, one can determine the distance from the production point and the decay point of the B-mesons. To determine the proper times distance, however, you need to measure the actual energy of the B-meson *and* the decay length at the same time.

7   Coulomb scattering

The case of Coulomb potential is somewhat special because the potential turn off at infinity rather slowly. In fact, the formalism we used so far assumed
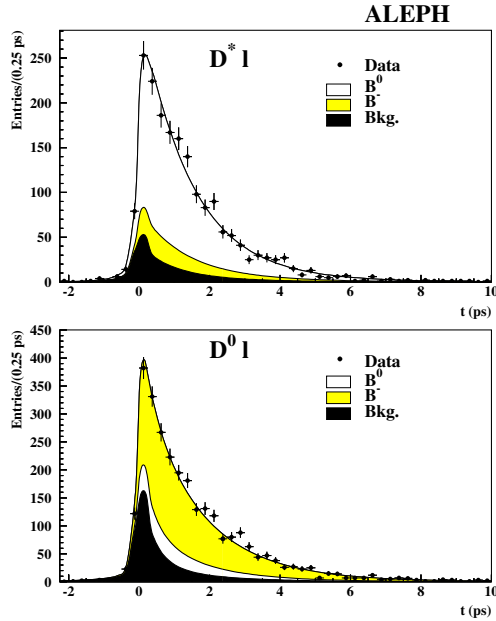
Figure 3: Measurement of B^0 and B^- meson lifetimes from $e^+e^- \rightarrow Z^0 \rightarrow b\bar{b}$, followed by formation of $B^{0,-}$ mesons due to quark confinement, and subsequent decay of the mesons. The decay of the mesons are detected by the modes $D^{*+}\ell^-$ and $D^0\ell^-$ seen in the detector away from the decay region and extrapolated back to the decay region. What are shown are proper time distributions for the $D^{*+}\ell^-$ and $D^0\ell^-$ samples, with the results of the fit superimposed. Also shown are the background contributions and the respective $\bar{B}^0$ and B^- components.

that the potential dies quickly enough to justify the asymptotic form

$$\psi(\vec{x}) \sim e^{ikz} + f(\theta)\frac{e^{ikr}}{r}. \tag{87}$$

This asymptotic behavior, however, is not valid for the Coulomb potential. Coulomb pontential is long-ranged and distorts the wave function even at large distances. In order to see this, we need to solve the equation exactly.

As usual, we go back to the Schödinger equation

$$\left[-\frac{\hbar^2}{2m}\Delta + \frac{ZZ'e^2}{r}\right]\psi(\vec{x}) = E\psi(\vec{x}). \tag{88}$$

We introduce some notations:

$$E = \frac{\hbar^2 k^2}{2m} = \frac{1}{2}mv^2 \qquad \left(v = \frac{\hbar k}{m}\right), \tag{89}$$

$$\gamma = \frac{ZZ'e^2}{\hbar v} = \frac{1}{ka_B} \qquad \left(a_B = \frac{\hbar^2}{ZZ'e^2 m}\right). \tag{90}$$

The dimensionless parameter γ controls the impact of the Coulomb field on the wave function. In terms of these quantities, the Schrödinger equation can be written much more simply as

$$\left[\Delta + k^2 - \frac{2\gamma k}{r}\right]\psi(\vec{x}) = 0. \tag{91}$$

To solve Eq. (91), we take the ansatz

$$\psi(\vec{x}) = e^{ikz}f(u), \qquad u = r - z. \tag{92}$$

By substituting the ansatz into Eq. (91), we find

$$u\frac{d^2}{du^2}f + (1 - iku)\frac{d}{du}f - \gamma k f = 0. \tag{93}$$

Introducing yet another variable $v = iku = ik(r - z)$, it becomes

$$v\frac{d^2}{dv^2}f + (1 - v)\frac{d}{dv}f + i\gamma f = 0. \tag{94}$$

24

This is a differential equation of Laplace-type and hence its solution is given in terms of a confluent hypergeometric function. Putting all pieces together, the solution is given as

$$\psi(\vec{x}) = Ae^{ikz}F(-i\gamma|1|ik(r-z)). \tag{95}$$

A is an arbitrary overall normalization factor. The exact solutions are sometimes called Coulomb harmonics.

Details of the hypergeometric functions are not of our interest. But we are interested in the asymptotic behavior of the function. By choosing the normalization factor $A = \Gamma(1+i\gamma)e^{-\pi\gamma/2}$ for convenience, the asymptotic behavior is given as

$$\begin{aligned}
\psi \quad \sim \quad & e^{i(kz+\gamma\log k(r-z))}\left[1 + \frac{\gamma^2}{ik(r-z)} + \cdots\right] \\
& -\frac{\gamma}{k(r-z)}\frac{\Gamma(1+i\gamma)}{\Gamma(1-i\gamma)}e^{i(kr-\gamma\log k(r-z))}\left[1 + \frac{(1+i\gamma)^2}{ik(r-z)} + \cdots\right].
\end{aligned} \tag{96}$$

The terms indicated by dots are suppressed by higher powers in $1/(r-z)$. Clearly this expression is not useful when $r = z$, $i.e.$, the extreme forward region. But as we discussed in "Scattering I," the scattering cross section does not deal with the forward region because it ignores the interference term. Therefore we will not worry about the subleading terms in $1/(r-z)$ and keep only the leading term 1 in the asymptotic expansion.

The asymptotic form of the wave function in Eq. (96) is not quite that in Eq. (87), but is similar enough to allow us to read off the scattering amplitude. We slightly modify the definition of the scattering amplitude from Eq. (87) as

$$\psi(\vec{x}) \sim e^{i(kz+\gamma\log k(r-z))} + f(\theta)\frac{e^{i(kr-\gamma\log k(r-z))}}{r}. \tag{97}$$

One can check, for example using wave packets, that this generalized definition still gives the probability of the particle to be scattered in a given solid angle. Comparing Eqs. (97) and (96), we find

$$f(\theta) = -\frac{\gamma}{k}\frac{\Gamma(1+i\gamma)}{\Gamma(1-i\gamma)}\frac{r}{r-z} = -\frac{\gamma}{k}\frac{\Gamma(1+i\gamma)}{\Gamma(1-i\gamma)}\frac{1}{2\sin^2\theta/2} \tag{98}$$

The scattering cross section is then obtained by the usual formula

$$\frac{d\sigma}{d\Omega} = |f(\theta)|^2 = \frac{\gamma^2}{4k^2\sin^4\theta/2} = \left(\frac{ZZ'e^2}{4E}\right)^2\frac{1}{\sin^4\theta/2}. \tag{99}$$

It is a coincidence that the Born approximation and the classical calculation both agree with this exact quantum mechanical result.

The fact that we did not have to worry about logarithmic correction in the exponents to obtain the scattering amplitude may make you wonder if the distortion of the wave function is of any physical significance. For the Rutherford scattering itself, certainly it does not matter. However, the distortion has importance consequences on other processes. One prime example is the nuclear β-decay. As well-known, nuclear β-decay transforms one type of nucleus with $A = N_p + N_n$, $Z = N_p$ to another one with the same A but a smaller atomic number $Z - 1$ by emitting an electron e^- and anti-electron-neutrino $\bar{\nu}_e$. When the β-electron escapes the nucleus, it is subject to the binding due to the Coulomb interaction. To calculate the decay matrix element, it is important to use Coulomb harmonics rather than plane waves.

Coming back to the scattering problem, now that we have the scattering amplitude, we can look for poles. Note that the Gamma function does not have zeros, and hence we look for poles of the numerator $\Gamma(1 + i\gamma)$. The poles of $\Gamma(z)$ are located at $z = 0, -1, -2, \cdots$, or in other words $-n + 1$ for $n = 1, 2, \cdots$. Therefore the poles are at

$$1 + i\gamma = -n + 1 \tag{100}$$

Recalling the definition of γ in Eq. (90), $\gamma = 1/ka_B$, we clearly need a pure imaginary k: bound states. To be in the physical region (upper half plane $k = i\kappa$ with $\kappa > 0$) to have an exponentially damping function at large radii, and to satisfy the condition Eq. (100), we need

$$\frac{1}{\kappa a_B} = -n, \tag{101}$$

or in other words a negative $a_B = \frac{\hbar^2}{ZZ'e^2m}$. It is possible only when $ZZ' < 0$, *i.e.* when the Coulomb potential is attractive. This is indeed what we expect. The energy levels are then obtained as

$$E = -\frac{\hbar^2\kappa^2}{2m} = -\frac{\hbar^2}{2ma_B^2n^2} = -\frac{Z^2Z'^2e^4m}{2\hbar^2n^2} = -\frac{Z^2Z'^2\alpha^2mc^2}{2n^2}. \tag{102}$$

This is nothing but the Bohr levels of hydrogen-like atoms as expected.

8   Two-to-two Scattering

We have discussed only the scattering of a particle by a static potential. In practice, a potential is generated by another particle, and we need to discuss two-to-two scattering problems. As long as the scattering is elastic, namely if the initial state particles and final state particles are the same, what we have done applies directly to realistic problems.

The point is just the separation of the center-of-mass motion in the two-body system. Starting from the two-particle Hamiltonian,

$$H = \frac{\vec{p}_1^2}{2m_1} + \frac{\vec{p}_2^2}{2m_2} + V(|\vec{x}_1 - \vec{x}_2|), \tag{103}$$

we separate the center-of-mass motion by defining

$$\vec{P} = \vec{p}_1 + \vec{p}_2, \qquad \vec{p} = \frac{1}{2}(\vec{p}_1 - \vec{p}_2),$$

$$\vec{X} = \frac{m_1\vec{x}_1 + m_2\vec{x}_2}{m_1 + m_2}, \qquad \vec{x} = \vec{x}_1 - \vec{x}_2. \tag{104}$$

Then the Hamiltonian becomes

$$H = \frac{\vec{P}^2}{2M} + \frac{\vec{p}^2}{2\mu} + V(|\vec{x}|), \tag{105}$$

with $M = m_1 + m_2$ and $\mu = m_1 m_2/(m_1 + m_2)$. Then the problem reduces to the potential scattering problem for a particle of mass μ.

There is, however, one interesting complication due to quantum statistics. If two particles that scatter are idential particles, such as electron-electron scattering or scattering of two idential atoms, symmetry of the wave function needs to be considered. Under the interchange of two particles $\vec{x}_1 \leftrightarrow \vec{x}_2$, $\vec{p}_1 \leftrightarrow \vec{p}_2$, the center of mass motion is not affected, but the relative coordinates change their signs $\vec{x} \leftrightarrow -\vec{x}$, $\vec{p} \leftrightarrow -\vec{p}$. If they have spins, their spins need to be interchanged at the same time.

If two particles are idential spinless bosons, say two Helium atoms (assuming ^{4}He isotopes), there is no spin degrees of freedom and the interchange of particles is simply $\vec{x} \rightarrow -\vec{x}$ in the wave function. Because they are bosons, the wave function should not change under the interchange of particles, and hence the wave function must be an even function of $\vec{x}$. Therefore the asymptotic form of the wave function Eq. (87) must be changed to

$$\psi(\vec{x}) \sim e^{ikz} + e^{-ikz} + [f(\theta) + f(\pi - \theta)]\frac{e^{ikr}}{r}. \tag{106}$$

27

The scattering amplitude $f(\theta)$ is calculated without the statistics in consideration, and the combination in the square bracket symmetrizes it. The differential cross section is then found to be

$$\frac{d\sigma}{d\Omega} = |f(\theta) + f(\pi - \theta)|^2. \tag{107}$$

There is a constructive interference at $\theta = \pi/2$ which can be experimentally observed. Note that one should not integrate over the entire solid angle to obtain the total cross section because (θ, ϕ) and $(\pi - \theta, \phi + \pi)$ correspond to an identical state:

$$\sigma = \int_0^{2\pi} d\phi \int_0^1 d\cos\theta \frac{d\sigma}{d\Omega}. \tag{108}$$

For two spin $1/2$ fermions, there are two possible spin wave functions, symmetric $S = 1$ and anti-symmetric $S = 0$. Therefore depending on the spin wave function, we either have a anti-symmetric or symmetric spatial wave function, respectively. In particular, the differential cross section is the same for the spinless bosons Eq. (107) for the anti-symmetric spin wave function $S = 0$, while it is

$$\frac{d\sigma}{d\Omega} = |f(\theta) - f(\pi - \theta)|^2 \tag{109}$$

for the symmetric spin wave function $S = 1$. In the latter case, the differential cross section vanishes identically at $\theta = \pi/2$. This is an interesting observation, and one can actually isolate $S = 1$ combination by studying $\theta = \pi/2$ region.

Many scattering phenomena of interest are inelastic, *i.e.*, the final state particles are not the same as the initial state particles. For instance, when an electron scatters off an atom, the final state atom may be in an excited state. Or one of the electrons bound to the atom may be kicked out from the atom. These are examples of inelastic scattering problems. We will not discuss these problems, but obviously the combination of elastic and inelastic processes will tell us a great deal about the nature of the object you study by scattering processes.

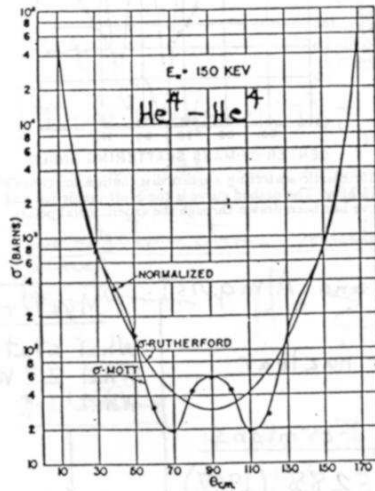N.P. Heydenberg and G.M. Temmer, Phys. Rev. 104, 123 (1956)

FIG. 4. Angular distribution of α—α scattering at 150 kev, our lowest energy. Data are normalized at 40° to the theoretical Mott curve. Differential cross section in the c.m. system in barns. Rutherford cross section is also shown (no interference term). This represents the most detailed confirmation of the influence of identity on scattering.
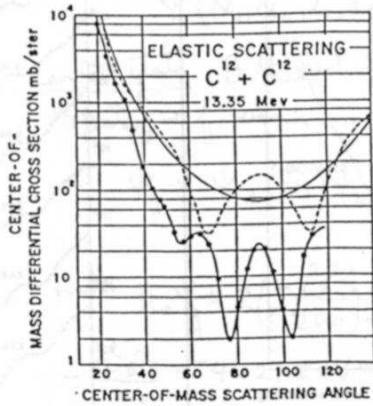
ELASTIC SCATTERING

OF IDENTICAL SPIN-ZERO NUCLEI

D.A. Bromley, J.A. Kuehner, and E. Almqvist, Phys. Rev. 123, 878 (1961)
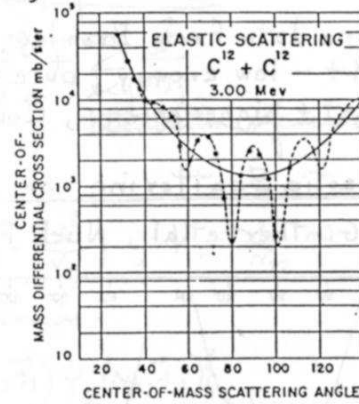
FIG. 7. Elastic scattering angular distribution for $C^{12}+C^{12}$ at $E_{c.m.} = 3.00$ Mev. The solid curve is the Rutherford prediction; the dashed curve is the Mott prediction. The spot diameters encompass the statistical counting errors.

FIG. 12. Elastic scattering angular distribution for $C^{12}+C^{12}$ at $E_{c.m.} = 13.35$ Mev. See caption to Fig. 7.

Above — energy low enough that only Coulomb force enters.

To Left — higher energy; nuclear and Coulomb forces enter. Interference pattern still symmetric about 90° and still with maximum there.

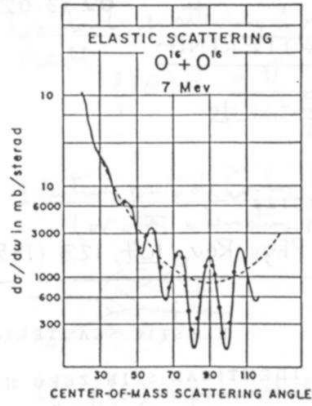Figure 4: Data on scattering of identical particles found by Prof. Dave Jackson.

29

FIG. 14. Elastic scattering angular distribution for $O^{16}+O^{16}$ at $E_{c.m.}=7$ Mev. The dashed curve is the Rutherford prediction and the solid curve the Mott prediction for the differential cross section. The spot diameter encompasses the statistical counting errors.
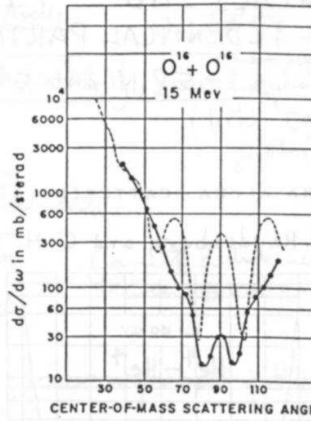
FIG. 18. Elastic scattering angular distribution for $O^{16}+O^{16}$ at $E_{c.m.}=15$ Mev. The dashed curve is the Mott prediction and the solid curve has been drawn through the experimental points.

More data from Bromley, Kuehner, and Almqvist.

Left — low energy, pure Coulomb

Right — higher energy, Coulomb plus nuclear

Mystery

What statistics?
What Z? What A?
What J?

Elastic Scattering of Identical Fermions

G. Günther et al., Nucl. Phys. A101, 288 (1967)
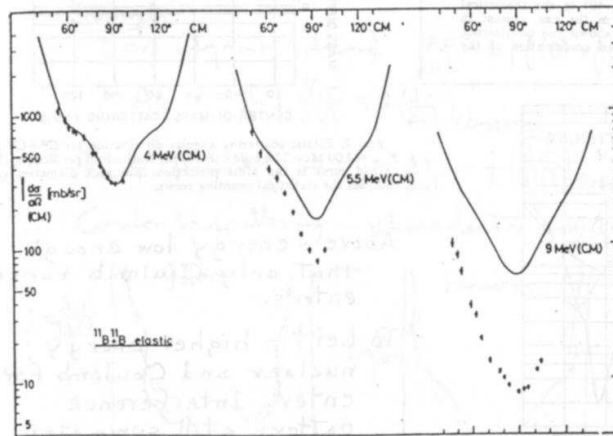
Fig. 5. Angular distributions measured at three energies. The solid lines represent Mott scattering.
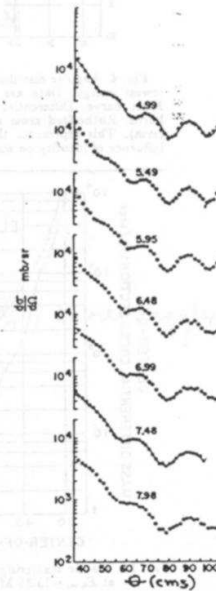
Figure 5: Data on scattering of identical particles found by Prof. Dave Jackson.

30